








Article

Fuzzy-Based Efficient Control of DC Microgrid Configuration for PV-Energized EV Charging Station

Dominic Savio Abraham ^{1,*}, Balaji Chandrasekar ¹, Narayanamoorthi Rajamanickam ¹, Pradeep Vishnuram ¹, Venkatesan Ramakrishnan ¹, Mohit Bajaj ^{2,3,4,*}, Marian Piecha ⁵, Vojtech Blazek ⁶ and Lukas Prokop ^{6,*}

¹ Department of Electrical and Electronics Engineering, SRM Institute of Science and Technology, Chennai 603203, India

² Department of Electrical Engineering, Graphic Era (Deemed to be University), Dehradun 248002, India

³ Graphic Era Hill University, Dehradun 248002, India

⁴ Applied Science Research Center, Applied Science Private University, Amman 11931, Jordan

⁵ Ministry of Industry and Trade, 11015 Prague, Czech Republic

⁶ ENET Centre, VSB—Technical University of Ostrava, 70800 Ostrava, Czech Republic

* Correspondence: agdominicsavio@gmail.com (D.S.A.); thebestbajaj@gmail.com (M.B.); lukas.prokop@vsb.cz (L.P.)

Abstract: Electric vehicles (EVs) are considered as the leading-edge form of mobility. However, the integration of electric vehicles with charging stations is a contentious issue. Managing the available grid power and bus voltage regulation is addressed through renewable energy. This work proposes a grid-connected photovoltaic (PV)-powered EV charging station with converter control technique. The controller unit is interfaced with the renewable energy source, bidirectional converter, and local energy storage unit (ESU). The bidirectional converter provides a regulated output with a fuzzy logic controller (FLC) during charging and discharging. The fuzzy control is implemented to maintain a decentralized power distribution between the microgrid DC-link and ESU. The PV coupled to the DC microgrid of the charging station is variable in nature. Hence, the microgrid-based charging is examined under a range of realistic scenarios, including low, total PV power output and different state of charge (SOC) levels of ESU. In order to accomplish the effective charging of EV, a decentralized energy management system is created to control the energy flow among the PV system, the battery, and the grid. The proposed controller's effectiveness is validated using a simulation have been analyzed using MATLAB under various microgrid situations. Additionally, the experimental results are validated under various modes of operation.

Keywords: electric vehicle (EV); level-1 EV charging station; bidirectional converter; fuzzy logic control



Citation: Abraham, D.S.; Chandrasekar, B.; Rajamanickam, N.; Vishnuram, P.; Ramakrishnan, V.; Bajaj, M.; Piecha, M.; Blazek, V.; Prokop, L. Fuzzy-Based Efficient Control of DC Microgrid Configuration for PV-Energized EV Charging Station. *Energies* **2023**, *16*, 2753. <https://doi.org/10.3390/en16062753>

Academic Editors: Pedro S. Moura and Ana Soares

Received: 4 March 2023

Revised: 13 March 2023

Accepted: 14 March 2023

Published: 15 March 2023



Copyright: © 2023 by the authors. Licensee MDPI, Basel, Switzerland. This article is an open access article distributed under the terms and conditions of the Creative Commons Attribution (CC BY) license (<https://creativecommons.org/licenses/by/4.0/>).

1. Introduction

Due to the depletion of fossil fuels and climate changes, the transportation sector has upgraded; electric vehicles play a significant role. The electrification of the electric vehicle (EV) battery depends on the grid condition. Thus, the renewable energy source (RES)-powered EV charging infrastructure and its effective utilization reduces charging costs and grid overload [1,2]. A photovoltaic (PV) system is the prime source of RES, which provides a standalone operation at all DC power requirement applications [3]. The RES-connected charging station offers a solution for power demand on the utility grid. However, the problems of the harmonics and voltage fluctuations in the utility grid system are balanced by the RES-powered balanced charging station [4–6]. Therefore, a microgrid with RES connected charging station provides an alternative to grid-connected charging.

A residential grid-connected charging station requires at least a four-power electronics converter. The first stage of the converter for PV integration with the DC bus requires

a DC–DC boost converter with high gain and control. The PV with a dedicated boost converter is used to power most commercial and residential EV charging applications. Fuzzy systems have been used in many scientific domains since they are simple to adapt to complicated procedures and do not require previous data as other intelligent controllers do. Fuzzy logic control has been used in this study due to these factors. Similar to how the charging station needs an energy management plan to manage power flow, vehicles benefit more from fuzzy-based optimization [7]. The EV, powered by the battery storage by RES, is more efficient and eco-friendlier when compared to other EV technologies [8,9]. The charging architecture of EVs can take supply from the DC microgrid or give supply to the DC microgrid through the bidirectional converter [10]. Reducing the stress in the utility grid and avoiding the usage of non-renewable sources, EVs act as power sources [11]. The EVs are charged from the DC bus; hence, it requires the second stage of the converter, which is the DC–DC buck converter [12]. The second stage of converters at the charging stations is DC–DC bidirectional converter (BDC) for ESU charging or discharging [13]. For grid-connected charging, and AC–DC rectifier is connected between the utility grid and the DC bus [14].

The EV is charged through the BDC. The advantages of using BDC are to support the power flow between the DC bus to the vehicle (G2V) and the vehicle to the DC bus (V2G) [15]. The BDC functions as a boost converter when the power is transferred from the low-voltage end to the high-voltage end. A typical block diagram of the charging station is shown in Figure 1. A charging station with a DC microgrid is supported by PV, ESU, and the utility grid. The bidirectional AC–DC converter connects the utility grid to the DC microgrid. The type of load connected to the DC bus determines the charging station's efficiency.

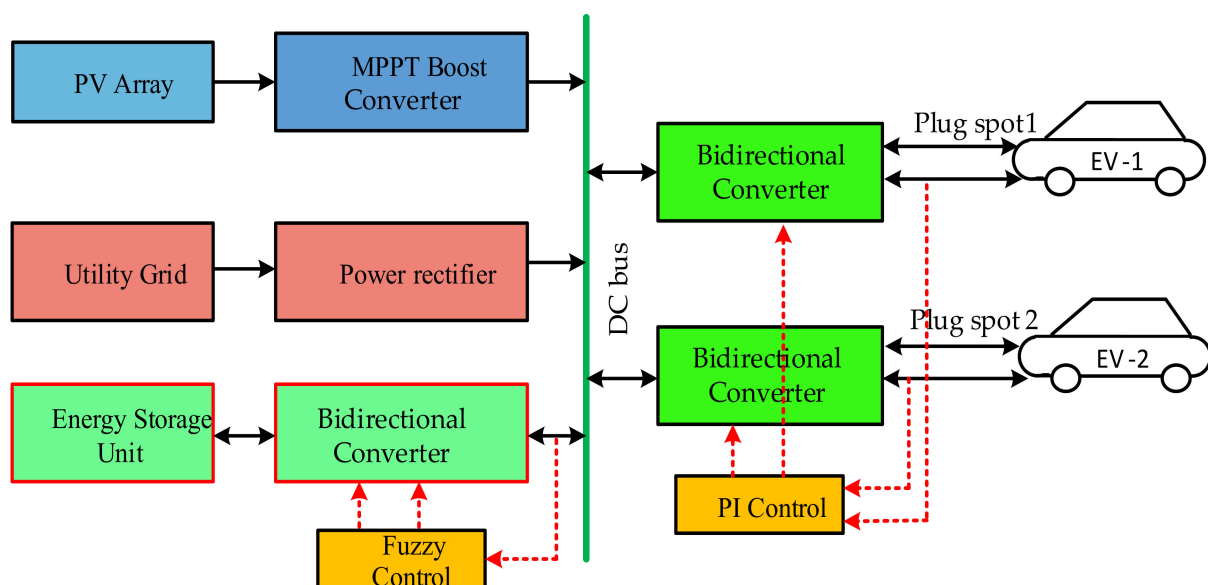


Figure 1. Fuzzy-controlled microgrid-based EV charging station.

The dual-stage architecture of the off-board EV charging station architecture is proposed; the first stage uses a maximum power point tracking (MPPT)-controlled DC–DC boost converter. Depending on the reference DC bus voltage, the controller is designed to provide a PWM signal to the DC–DC converter. When a large-scale signal is supplied, the proportional-integral (PI) controller cannot forecast the load voltage, which lengthens the rise time and dampens oscillation [16]. The charging stations are controlled through centralized control when the charging station is small [17]. The decentralized controller is more suitable when connected to different sources [18]. Battery and modular STATCOM with fuzzy controllers are also used with the DC link powered by the PV source [19,20]. Prioritization for ESU charging or discharging at the charging station is fluid [21,22]. An-

other useful tool for controlling the power converter at the charging station is a fuzzy logic controller. The FLC goal in this study is to enable coordinated operation between the DC bus voltage and the energy storage unit's SOC (ESU). The primary innovation of this paper, in comparison to previous ones, is the use of fuzzy controllers as a decentralized EMS to independently control the converters of two system components and achieve coordinated operation of the following parameters: power flow, medium voltage direct current (MVDC), and energy storage unit (BESS) SOC.

The structure of this paper is as follows: Section 2 describes how the microgrid is configured for the EV charging station. Additionally, this section presents the proposed charging station architecture and its FLC control strategy for the ESU and bidirectional converter control. Section 3 is the detailed simulation analysis of the proposed charging station using MATLAB. The corresponding results are practically tested using the lab-based prototype in Section 4. Section 5 concludes this article.

2. Proposed Microgrid for EV Charging Station and Its Control

The proposed DC microgrid-based EV charging infrastructure contains a PV MPPT boost converter and BDC for connecting EV and ESU with the DC bus [23]. The DC bus in the microgrid is powered through the PV using a DC–DC boost converter and a utility grid using the bidirectional inverter. Depending on the solar irradiation, PV can deliver the range of the power output [24]. The energy storage unit stores the charge for future usage and provides an uninterrupted supply for charging. The PV-powered EV charging infrastructure is shown in Figure 2.

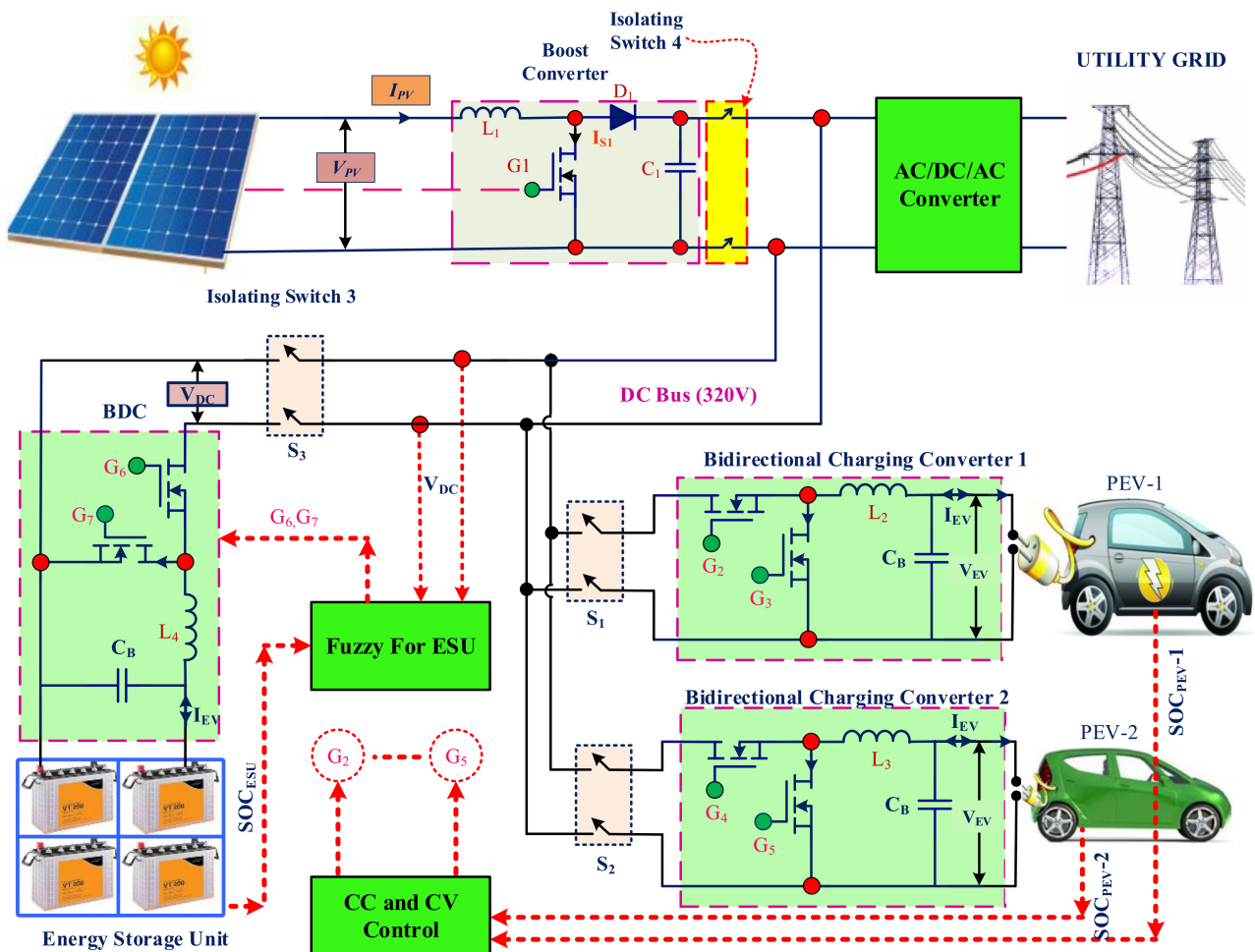


Figure 2. DC microgrid-based bidirectional EV charging station architecture.

The charging station operated in different modes based on the requirement of the charging station. Generally, the EV charging is performed through a renewable energy source, when the RES cannot power the charging station or is charged from the EV, the ESU, and the utility grid. During the operation of PV to EV, the utility grid, and the ESU-based charging mode, it is necessary to regulate the DC bus voltage [25,26]. The DC-to-DC converter interfaces with the PV and the DC bus and uses maximum power point tracking (MPPT) to utilize PV power effectively. The ESU regulates the DC bus voltage through the fuzzy logic controller. The BDC operates in a boost mode when the arrived vehicle is fully charged and is ready to transfer the power to the charging station storage [27]. The EV's full charge is identified by measuring the SOC values of the battery inside the vehicle [28,29]. The reference value of SOC for vehicle-to-vehicle (V2V) mode is 60% [30]. The half bridge BDC operates as a buck mode during the charging mode to provide increased current for fast charging [31,32]. An FLC controller using goal representation adaptive dynamic programming is used to improve the stability of system photovoltaics. The literature also discusses coordinated charging, which is a potential way to lessen the effect of recharging EVs on the distribution grid network to which they are attached.

The proposed dual-stage charging station provides the option for V2V also. The characteristics and advantages of the DC bus-connected EV charging station are as follows:

- This charging station can operate independently without receiving power from the utility grid; the development of a ESU2G system includes the development of an appropriate regulated power to the DC microgrid.
- A battery used as an EV provides a continuous supply to the EV charging terminals with its PI control.

The direct level-1 EV charging station consists of three different converters: A boost converter from the renewable energy source side, a bidirectional converter from the vehicle side, and an inverter for utility grid integration. The charging station is connected to different types of loads. The different loads depend on road transportation; electric bikes, e-rickshaws, and EVs are connected to the charging station. Based on the battery capacity, the charging station can control its charging. With the FLC control strategy, the bidirectional converter provides a regulated voltage to the DC bus and provides controlled charging for different types of electric vehicles.

2.1. Fuzzy Logic Control in ESU

The independent fuzzy logic control was developed to control the BDC in the vehicle and ESU side [33]. Using established procedures and knowledge, all DC loads in the public charging station were connected to the standard DC bus voltage levels for DC microgrids in residential buildings that were located between a distributed generator and the loads. Voltage values ranging from 12 V to 800 V have been suggested in the literature due to a lack of standardizations. In order to simplify the systems and cut losses, standard voltage levels for DC distribution systems are created. The present typical voltage values of 300–400 V electric vehicles may serve as inspiration for these DC voltage levels, even though some efforts are still being made to build these standards, based on the above criteria DC bus voltage is set as 320 V [34].

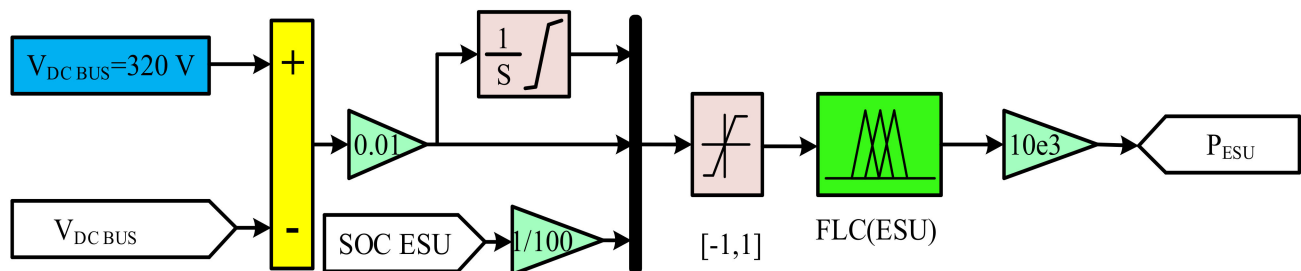
The different energy storage system with the renewable energy source-connected EV charging station DC bus voltage are controlled through the distributed bus signaling (DBS) method. A particle swarm optimization (PSO)-based approach is used in the EV charging station [35]. Decentralized energy sources in an EV charging station allow easy integration of power sources by forming a medium voltage microgrid [36].

This control strategy aims to provide the regulated output to the DC bus through ESU. The comparative analysis of the literature studies is provided in Table 1. The proposed fuzzy controller permits a good response, according to the comparison analysis. The quickness, stability, and dependability of the system will improve.

Table 1. Different fuzzy logic control at the charging.

Ref. No.	Controller Proposed	Contribution of the Work
[37]	FLC	AC microgrid voltage and frequency under different system load operations and different solar irradiation
[38]	Droop Control	Energy management system algorithm for a residential hybrid microgrid system and a real-time monitoring platform
[39]	FLC	The fuzzy-based scheme enables the storage to charge or discharge within the safe operating region.
[40]	FLC	Making the best choice feasible with the aid of a fuzzy logic controller to deal with smart charging.
[41]	FLC	Reduced steady state error response time of the charging station

For the control strategies, the output power is considered as the reference for the EV and ESU side power converters. The main objective of the fuzzy logic controller is to control DC bus voltage and SOC ESU. The fuzzy logic controller used for the ESU is shown in Figure 3.

**Figure 3.** FLC for ESU power control.

The following inputs are given to the fuzzy controller SOC_{ESU} , the cumulative error of DC bus voltage. The rated DC bus voltage is set as 320 V; the error is calculated by comparing the measured value with the reference. The error and the differential error of the inputs are taken as the normalized value between -1 and 1 ; this corresponds to the -30 V and $+30$ V. The SOC_{ESU} is the normalized value for fuzzy between 0 and 1 . There are seven membership functions assigned for the error and cumulative error: Negative high (NH), negative medium (NM), negative low (NL), zero (Z), positive low (PL), positive medium (PM), and positive high (PH) are shown in Figure 4a. The membership function of other input is SOC_{ESU} and rangers are assigned as low (L), medium (M), and high (H) is shown in Figure 4b. Based on the above input fuzzy values, ESU power is normalized between -1 and $+1$. The fuzzy membership function of P_{ESU} is assigned as negative high (NH), negative medium (NM), negative low (NL), zero (Z), positive low (PL), positive medium (PM), and positive high (PH) and is shown in Figure 4c. The ESU connected to the charging station is charged when the SOC values are low. The charging is considered unfavorable. The ESU delivered the power to the charging station when the SOC was medium, high value, and the discharging was positive.

The rule base of the fuzzy logic controller is developed based on the ESU SOC, and the corresponding is shown in Tables 2–4. The control differs based on the ion of the SOC level; when the SOC is high, the ESU is able to supply the power to the DC bus to provide the deficiency. During the time of discharge, ESU power is positive; similarly, when the value of SOC is low, ESU charged from the DC bus is considered as negative.

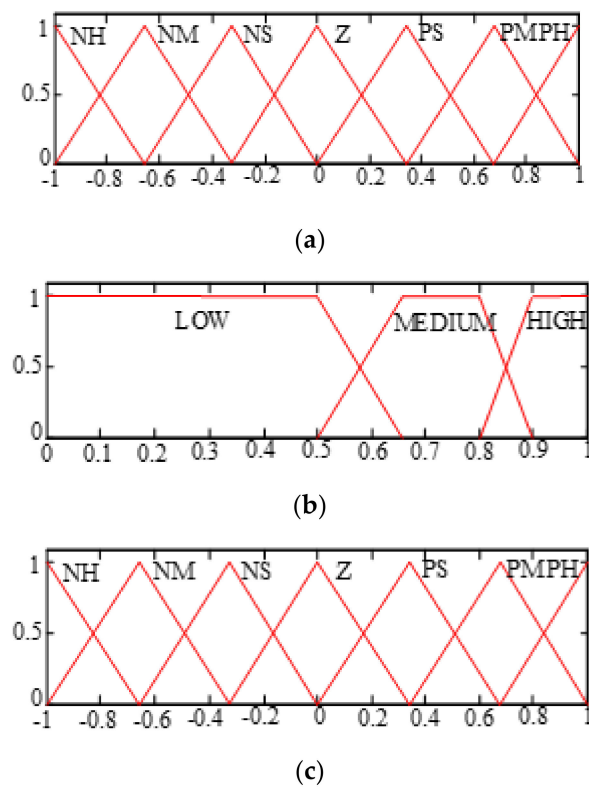


Figure 4. Membership function of input and output: (a) P_{ESU} , error and cumulative error; (b) SOC_{ESU} (c) P_{ESU} .

Table 2. Fuzzy rule base: P_{ESU} when SOC of ESU is low.

		Error						
		NH	NM	NS	Z	PS	PM	PH
Difference in Error	NH	NH	NH	NM	NM	NS	NS	Z
	NM	NH	NM	NM	NM	NM	NS	Z
	NS	NH	NM	NS	NS	NS	Z	Z
	Z	NH	NM	NS	Z	Z	Z	Z
	PS	NM	NM	NS	Z	Z	Z	Z
	PM	NS	NS	Z	Z	Z	Z	Z
	PH	Z	Z	Z	Z	Z	Z	Z

Table 3. Fuzzy rule base: P_{ESU} when SOC of ESU is medium.

		Error						
		NH	NM	NS	Z	PS	PM	PH
Difference in Error	NH	NH	NH	NM	NM	NS	NS	Z
	NS	NH	NM	NM	NM	NM	NS	PS
	NS	NH	NM	NS	NS	NS	Z	PS
	Z	NH	NM	NS	Z	Z	PS	PM
	PS	NM	NM	NS	Z	PS	PM	PH
	PM	NS	NS	Z	PS	PM	PH	PH
	PH	PH	Z	PS	PM	PH	PH	PH

Table 4. Fuzzy rule base: P_{ESU} when SOC of ESU is high.

		Error						
		NH	NM	NS	Z	PS	PM	PH
Difference in Error	NH	Z	Z	Z	Z	Z	Z	Z
	NS	Z	Z	Z	Z	Z	PS	PM
	NS	Z	Z	Z	Z	Z	Z	PM
	Z	Z	Z	Z	Z	PS	PM	PM
	PS	Z	Z	Z	PS	PM	PM	PH
	PM	Z	PS	PS	PM	PM	PH	PH
	PH	Z	PS	PM	PM	PH	PH	PH

A fluctuation in the DC bus voltage caused by fuzzy logic control grid management is required, and its controller rules are designed with this foundation.

2.2. Bidirectional Converter and its Control

The EV battery charging input power is given to the battery through the bidirectional converter. It operates in both boost and buck mode. The basic half-bridge bidirectional converter is operation in continuous conduction mode (CCM). The different converter used for the EV battery charging the bidirectional converter operates in boost and buck modes. The converter operates in buck mode during ESU charging or boosts while ESU supplies power to the charging station.

During charging, the charger follows a constant current and voltage charging, and the duty ratio d_v controls the buck mode operation of the charger, as shown in Figure 5.

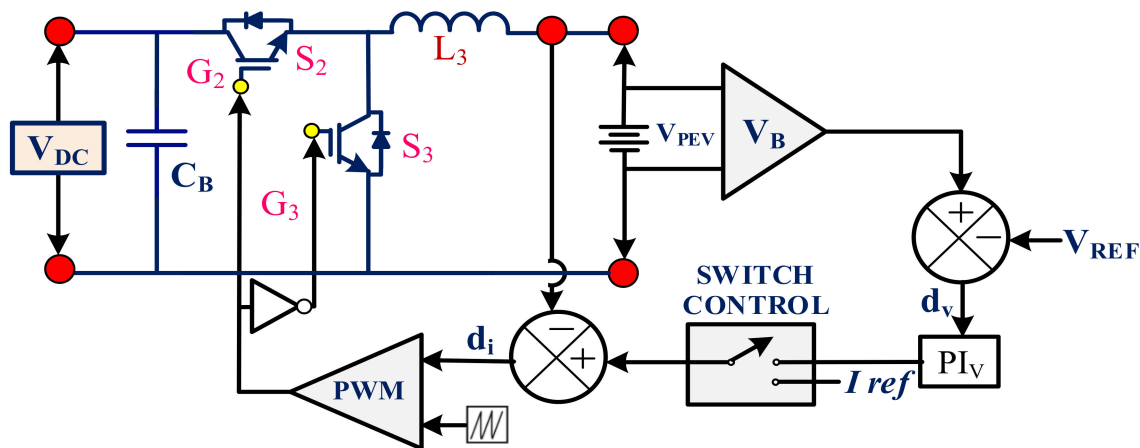


Figure 5. Bidirectional converter constant current (CC) and constant voltage (CV) control mechanisms for charging an EV battery.

The EV battery is charged by giving the charging converter a constant voltage and constant current control. Figure 6 illustrates how constant voltage charging is performed using an external voltage loop control and fast charging with an inner current loop control. The battery is charged if the current flowing into it is positive ($I_{batt} > 0$); otherwise, it is discharged. The energy management controller supplies the battery with a controlled supply based on the battery current's sign (I_{ref}). The battery is charged if $I_{ref} > 0$ and drained if $I_{ref} < 0$.

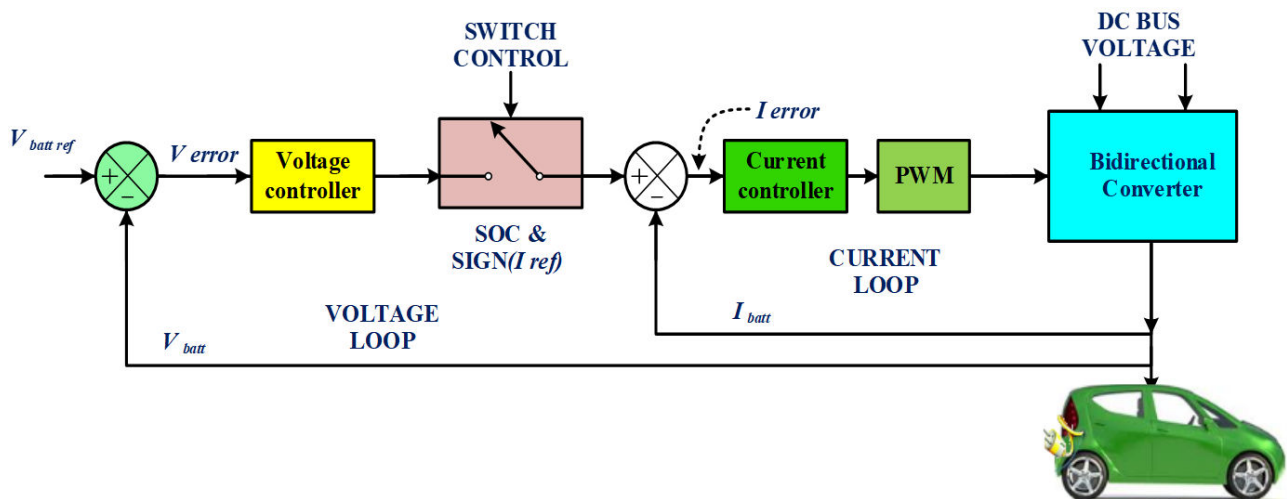


Figure 6. Controller for an EV battery.

A charging converter operating mode changes based on the SOC and sign of the reference current (I_{ref}). Depending on the switch control signal, it can be operated in either the constant voltage or constant current mode. When the switch is open, the charging station converter operates in constant current charging mode; when it is closed, it operates in constant voltage charging mode. This charging controller operates in two loops; the first loop is the faster current loop control, and the second loop is the outer voltage loop control. Based on the battery reference voltage and reference current, it can operate in constant current and constant voltage mode. If the EV battery SOC is less than 70% charging, the converter operates in constant current mode. Otherwise, it will be operated in constant voltage mode. In addition, bidirectional converter efficiency is increased through regulated charging and discharging of the current.

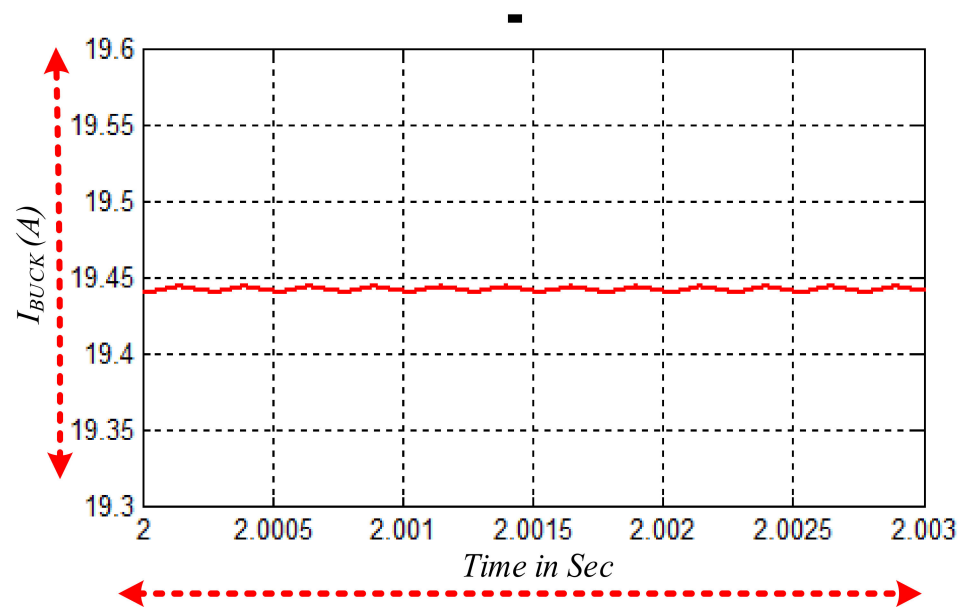
3. Simulation Results

PV of 5 kW is used to power the DC bus to charge the EV and 33 kVA energy storage unit and the electric vehicle at the charging station. The DC microgrid of 10 kW modelled in MATLAB/Simulink corresponding topology is depicted in Figure 2. The charging station consists of PV, utility grid, and ESU that are used as the primary sources for supplying the charging power. Considering the variations in SOC of ESU, the series of events that characterize the microgrid operation is simulated. Simulation parameters of the charging station taken for the simulation are given in Table 5. The fuzzy logic controller is implemented, and the corresponding gains are determined using the standard linearization procedure.

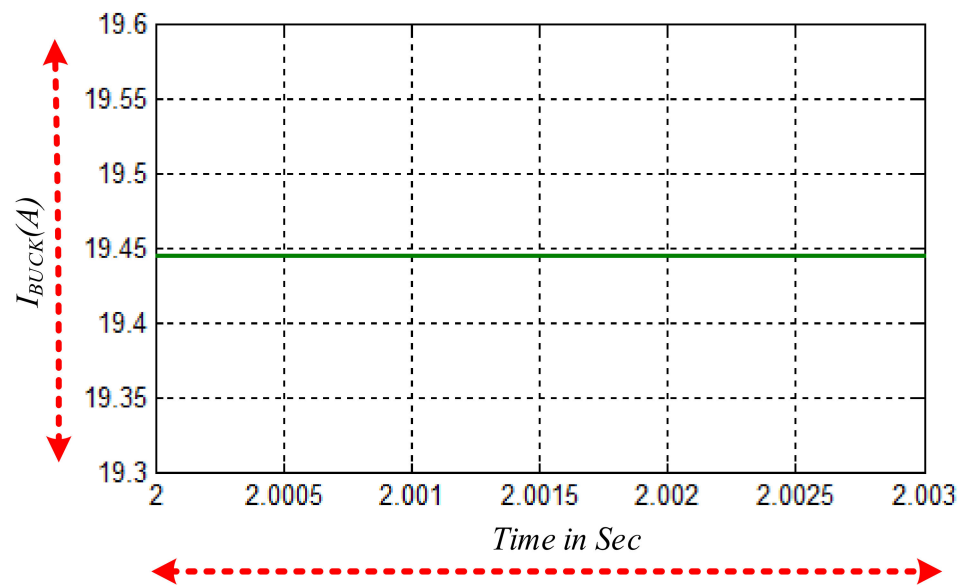
Table 5. Simulation parameters.

Parameters	Value	Unit
Utility grid voltage (E_{grid})	440	Vrms
DC bus capacitance (C_{DC-Bus})	1000	μF
PV power (P_{PV})	5000	W
DC bus voltage	320	V
EV battery power	1.0–6.6	kW
EV battery voltage	48	V
Power ESU	33	kW
ESU voltage	48	V
Maximum output current	20	A
Peak efficiency	96%	%

During PV to EV charging mode, charging is achieved by providing regulated voltage and current to the EV battery when the PV produces an output of 2 kW due to moderate irradiation. During this condition, DC bus obtains the power of 1.9 kW ($\pm 5\%$), and 320 V, 5.5 A and is regulated in the DC microgrid. The regulated output voltage of 320 V is maintained at the DC bus and is used to charge the EV. The charging current with reduced ripple is shown in Figure 7b. The regulated output achieved through the controller is operated to charge the EV battery under constant current and constant voltage charging, while maintaining DC bus voltage from the ESU fuzzy controller provides a faster settling time. Without a fuzzy controller, the settling time was observed as 0.8 s, while the fuzzy controller settling time was observed as 0.3 s.



(a)



(b)

Figure 7. Simulation output of charger output current: (a) Without fuzzy controller; (b) with fuzzy controller.

The DC bus mainly utilizes the power from the PV and ESU, because of the charging of EV mainly uses RES. During various values of SOC of the ESU, the DC bus voltages are analyzed for system performance. When the SOC of ESU is zero ($ESU_{SOC} = 0\%$) and the DC bus voltage of 325 V is measured due to the PV source, the DC bus voltage is maintained at 319 V during 0 to 1 s. The DC bus voltage is dropped during 1 to 2 s, and the PV is turned off; the DC bus voltage is dropped below the required DC bus voltage from 2 to 3 s. After three seconds, the ESU and PV sources are turned on, returning to the stable 322 V state and maintaining their voltage stability. Similarly, the different values of SOC of ESU are demonstrated and shown in Figure 8.

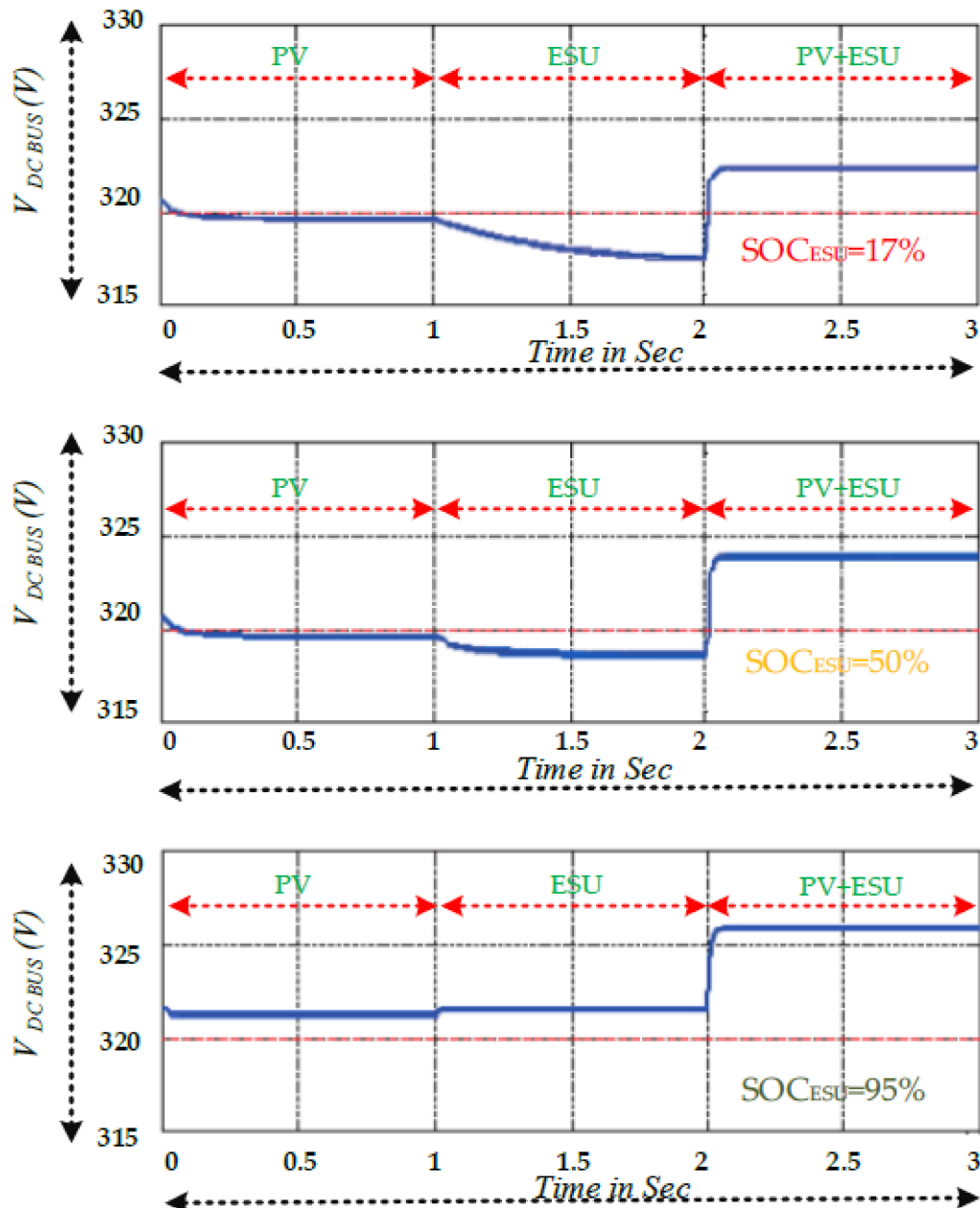


Figure 8. DC bus voltage at different values of SOC of ESU.

During vehicle charging, BDC operates in buck mode. During level one charging, PV voltage is given as 5 kW and is shown in Figure 9a. The MPPT-controlled PV-connected DC/DC converter is connected to the DC bus. The DC bus voltage is maintained as a regulated ripple-free value of 320 V. The EV connected to the DC bus with a SOC value of

59% is shown in Figure 9a. The bidirectional converter that is connected will be operated in buck mode to charge the EV, which gives the output voltage of 48 V, as shown in Figure 9a. When EV to ESU is in supply mode, the corresponding output values are shown in Figure 10b; the corresponding vehicle discharge voltage and DC bus voltage are maintained as 300 V while ESU power is measured as 1.2 kW.

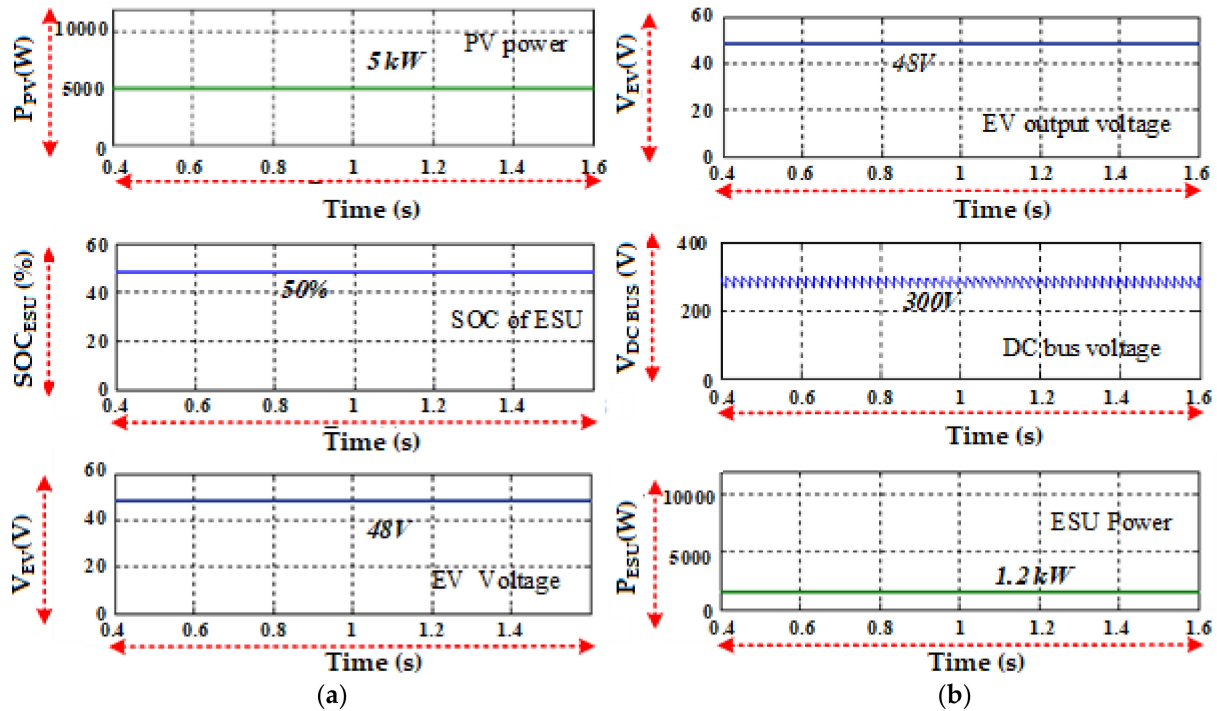


Figure 9. (a) PV to EV charging mode; (b) EV to ESU charging mode.

During the condition of utility grid overloaded, PV is not producing any output, and the SOC value of EV available at the charging station is above 90%; the EV battery supplies the power to the DC microgrid. The EV battery supplies the power to other EVs, and the corresponding output is shown in Figure 10a. When PV and ESU values are less than the reference level or cannot supply the power to the charging station, EV is charged from the utility grid, and the corresponding output is shown in Figure 10b.

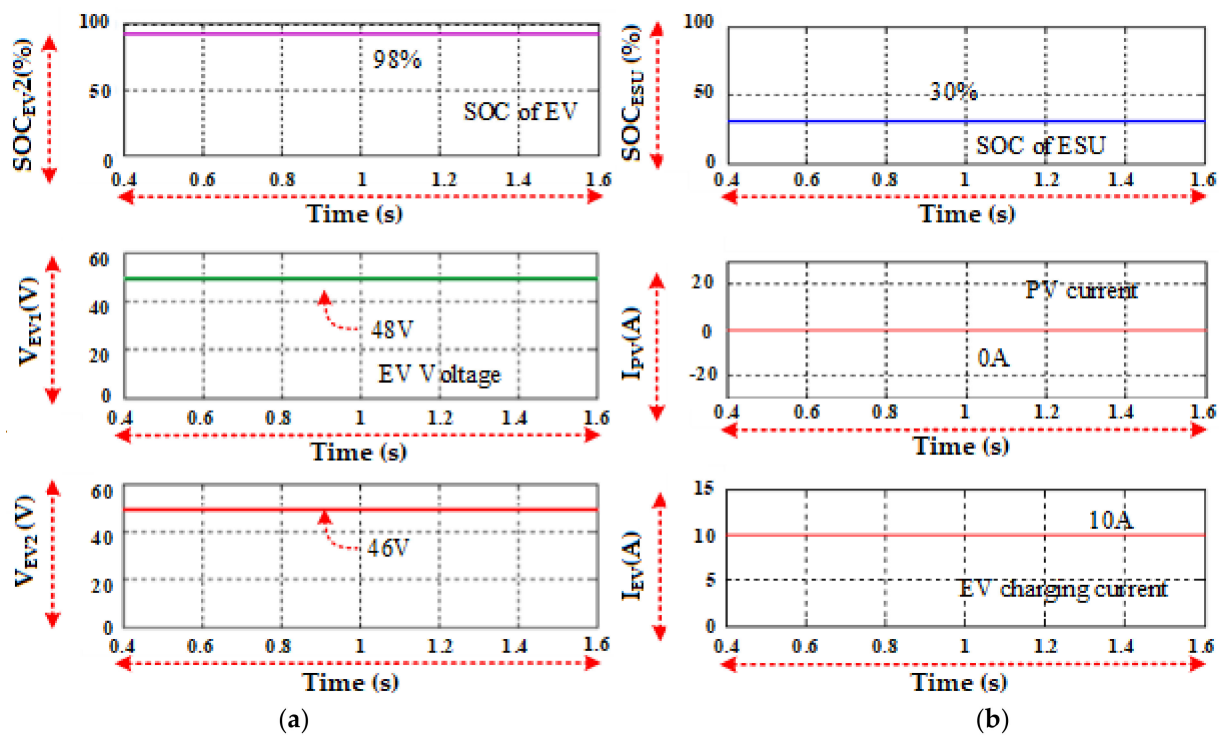


Figure 10. (a) EV 2 to EV 1 charging mod; (b) ESU to EV charging mode.

From the simulation results, the proposed level-1 standalone charging station is operated regardless of the various value of SOC of ESU. Based on the different modes of the power flow at the charging station, the measured values and summarized simulation results are shown in Table 6.

Table 6. Simulation results.

CS Parameters	PV to EV	EV to ESU	EV 2 to EV 1	ESU to EV
SOC_{ESU} (%)	50	30	30	30
SOC_{EV1} (%)	40	80	35	40
SOC_{EV2} (%)	60	90	90	85
V_{EV1} (V)	48	48	46	48
V_{EV2} (V)	48	48	48	48
$V_{DC\ BUS}$ (V)	320	300	300	320

As can be seen, the decentralized nature of the proposal control mechanism prevents the information from being sent between the DC/DC converters, and the DC bus's voltage level determines the charging station's working point. The DC microgrid-based charging station worked independently from the source, and the management of sources is performed based on the DC bus voltage. It is observed that the DC bus voltage is regulated in all cases.

4. Hardware Implementation

The experimental validation of the proposed off-board charging topology of a laboratory prototype is shown in Figure 11. The proposed charging station uses a PV of 240 W (18 V, 13.34 A) to charge the ESU of 48 V and 50 Ah and two EV of an EV battery capacity selected as $V_{EV} = 48$ V, $I_{EV} = 3.5$ A through the converter topology. The specification of the experimentally validated charging station is shown in Table 7. The experimental results were obtained in a laboratory environment for both DC–DC converters.

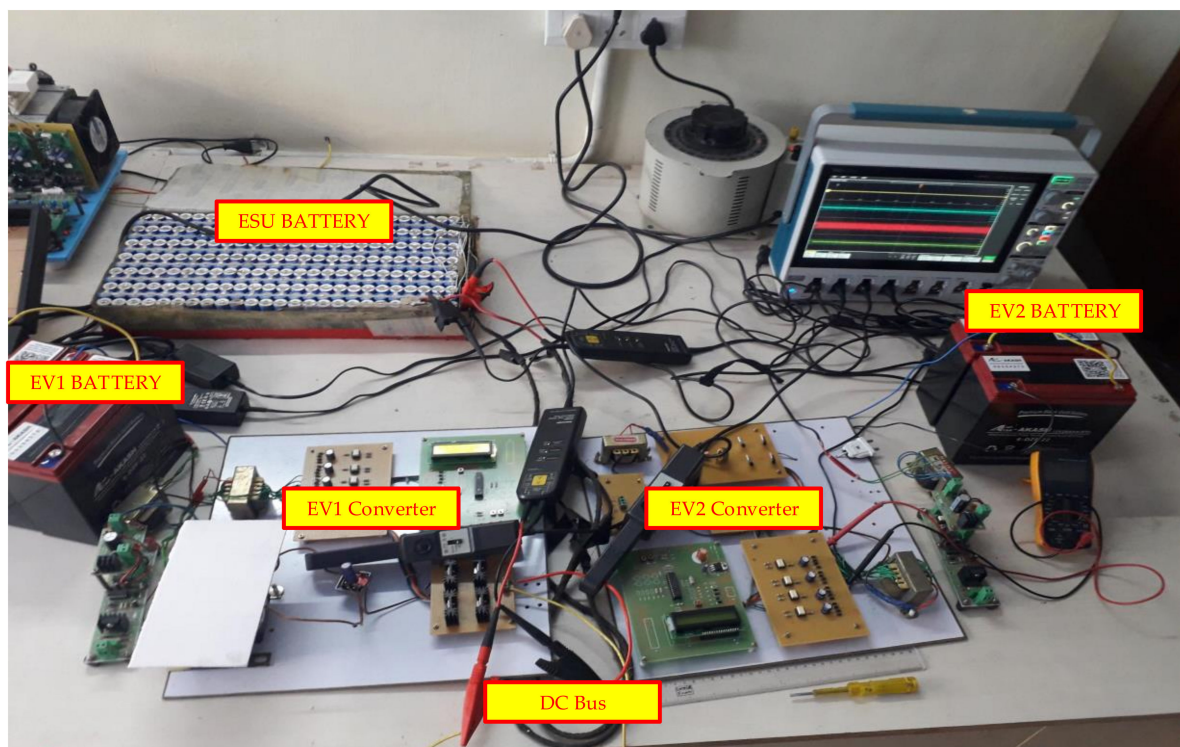
Table 7. Parameter of the experimental setup.

Parameters	Bidirectional Converter
Input voltage	320 V
Output voltage	48 V
Output power	230 W
Switching frequency	18 kHz
Duty—cycle	80%

The Li-ion battery used for vehicle storage and the parameters of the battery pack used in the experimental setup are shown in Table 8 and highlighted in red in Figure 11.

Table 8. Parameters of Li-ion battery as ESU.

Parameters	Value
Number of cells used	325
Number of cells in a row	25
Number of rows	13
Nominal voltage	48 V
Maximum voltage (charge mode)	52.1 V
Nominal capacity	50 Ah

**Figure 11.** Experimental setup.

In the dual-stage charging station, PV delivers the power with the maximum output of the PV panel, which is 220 W ($V_{PV} = 18$ V, $I_{PV} = 12.3$ A). The DC bus voltage is maintained at 220 V by supplying power by the PV alone using the DC/DC converter. The output of the EV side-charging bidirectional converter under buck mode is maintained at $V_{EV} = 48$ V, $I_{EV} = 3.5$ A and is shown in Figure 12a.

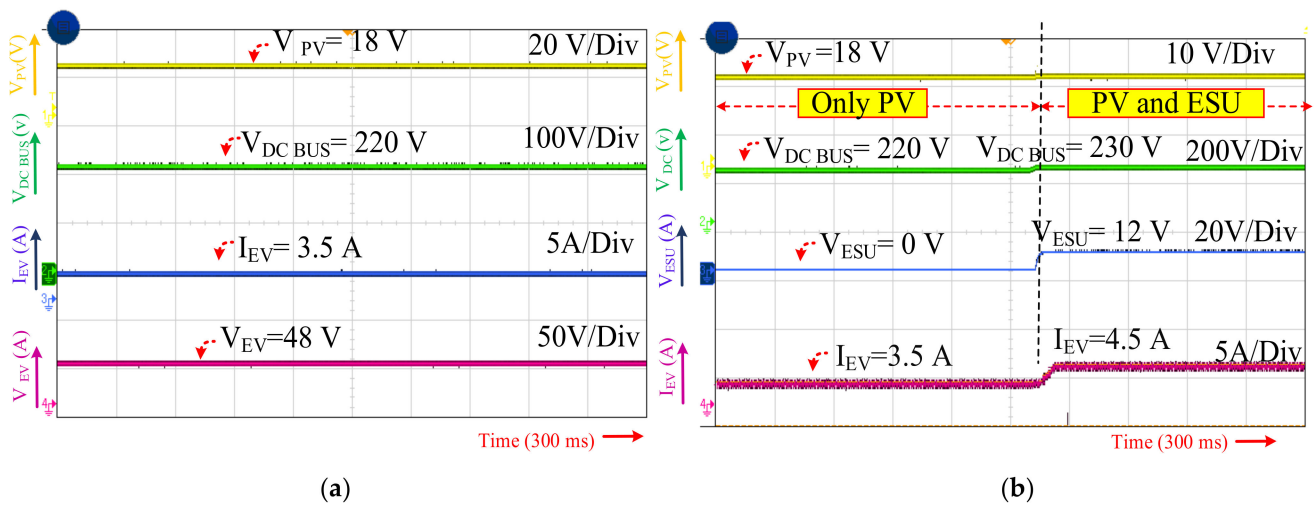


Figure 12. (a) PV to EV charging mode; (b) PV and ESU to EV charging source.

At the time different sources, such as PV and ESU, power a charging station, the DC bus voltage is measured as 220 V to 230 V at a given PV input of 18 V, and the corresponding value of ESU is changed 0 V to 12 V. During the time of different sources charging EV, the charging current is maintained based on the required value.

The experimental results in a single-phase grid utility grid to vehicle mode are shown in Figure 13a. It is observed that the G2V mode microgrid current is measured as 6 A; this is used to charge with the current of 5 A. The utility grid is connected with the source current of the total harmonic distortion of 3.5% and a power factor of 0.9. In addition, a utility grid during overloading conditions without ESU supply is shown in Figure 13b.

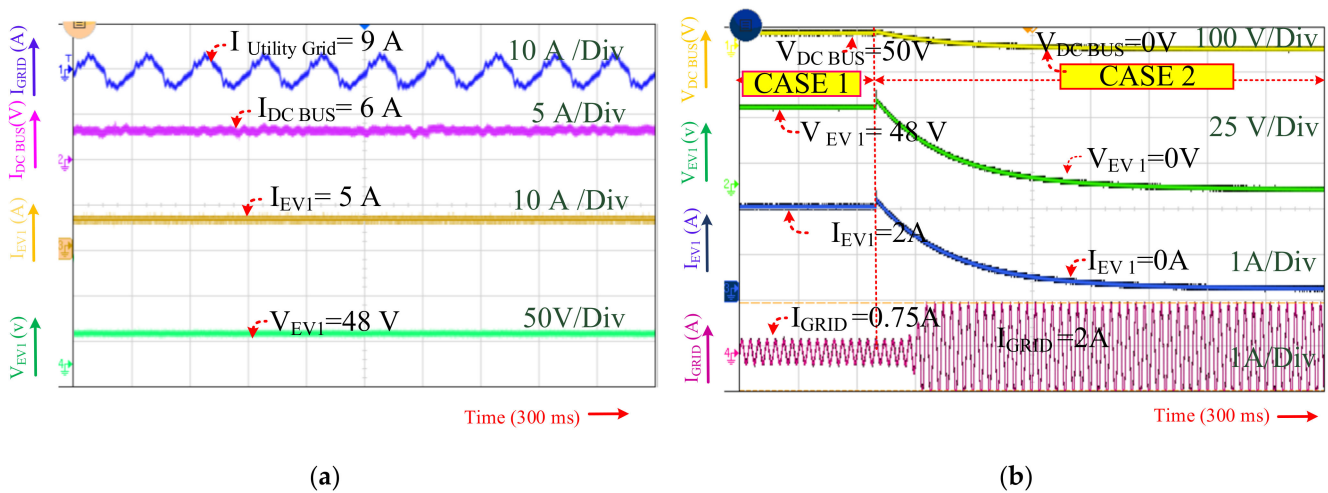


Figure 13. Experimental result: (a) Utility grid to EV mode; (b) different utility grid condition.

Microgrid voltage is measured at different utility grid conditions: when the grid is not overloaded, and when the utility grid is overloaded, the charging station cannot receive any power from the grid. When the utility grid is deficient in supplying the power, the charging ESU and EV supply the power for charging.

The efficiency of the proposed charging station has achieved a maximum of 95% with an increasing power input. The output power is taken from the charging station ranging between 130 W to 240 W and is considered for efficiency calculation. The proposed FLC controller provides the charging control with lesser commutation loss and ripple-free output for the continuous charging profile. The efficiency of the charging station is

graphically represented in Figure 14a. The percentage of charge and the corresponding voltage is shown in Figure 14b.

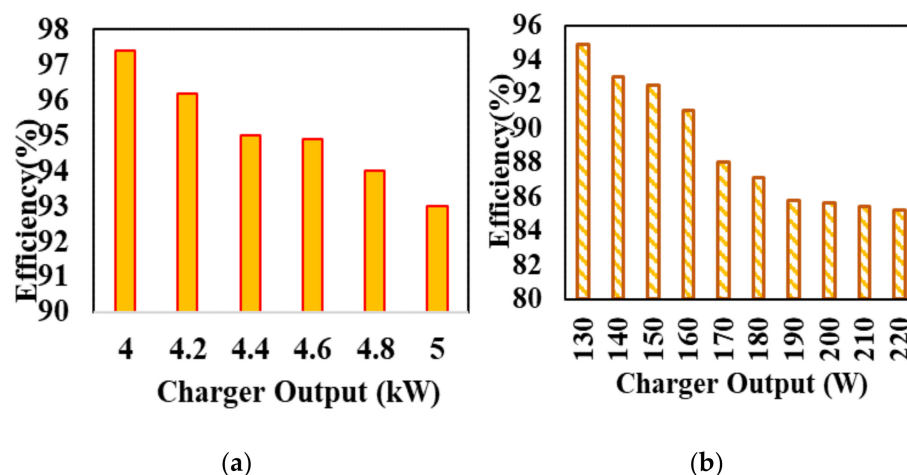


Figure 14. The efficiency of charging station: (a) Simulation; (b) hardware.

The efficiency of the charging station was achieved at 95 percent as experimentally under the level-1 charging. The efficiency through simulation study has been calculated at 97.4 percent at maximum power conditions.

5. Conclusions

The proposed EV charging station in the DC microgrid is designed with a PV array and a local energy storage unit to provide an uninterrupted and reliable power supply. In this work, to guarantee reliable charging, two control strategies are designed to control the grid's DC bus voltage and manage the available power to the EV charging plug spot. The fuzzy logic controller regulates ESU's charging/discharging voltage through the bidirectional converter to facilitate the charging requirements. An intelligent charging station has been developed based on fuzzy logic control, which is the bidirectional power flow between EVs' batteries and the grid during peak, standard, and off-peak hours. The overall control strategies are handled under various practical conditions, such as low irradiance of PV and single-phase utility grid overloading. The MATLAB simulation model designed for higher power rating, hardware implementation of a charging system with high gain boost, and a bidirectional converter provides better voltage regulation and improvement in charging rates. In addition, the laboratory-scale experimental prototype results are matched with simulation outcomes.

Author Contributions: Conceptualization, D.S.A., B.C. and P.V.; methodology, N.R.; software, M.B.; validation, D.S.A., N.R., V.R. and P.V.; formal analysis, V.B., L.P. and M.P.; investigation, M.B.; resources, L.P.; data curation, V.B.; writing—original draft preparation, D.S.A., P.V. and N.R.; writing—review and editing, D.S.A., P.V. and N.R.; visualization, M.B., V.B., L.P. and M.P.; supervision, V.B.; project administration, L.P.; funding acquisition, V.B., L.P., M.P. All authors listed have made a substantial, direct, and intellectual contribution to the work and approved it for publication. All authors have read and agreed to the published version of the manuscript.

Funding: This paper was supported by the following projects: VSB-TU Ostrava, project TN02000025 "National Centre for Energy II", and project CK04000060 "Developing analytical tools for an effective transition to electromobility" and Government of India, Department of Science and Technology (DST) Science and Engineering Research Board (SERB) Core Research Grant C.R.G./2020/004073.

Data Availability Statement: Not applicable.

Conflicts of Interest: The authors declare no conflict of interest.

References

1. Kraiem, H.; Flah, A.; Mohamed, N.; Alowaidi, M.; Bajaj, M.; Mishra, S.; Sharma, N.K.; Sharma, S.K. Increasing Electric Vehicle Autonomy Using a Photovoltaic System Controlled by Particle Swarm Optimization. *IEEE Access* **2021**, *9*, 72040–72054. [[CrossRef](#)]
2. Belik, M. Passive solar systems enhanced efficiency. *Renew. Energy Power Qual. J.* **2019**, *17*, 235–239. [[CrossRef](#)]
3. Dogga, R.; Pathak, M.K. Recent trends in solar PV inverter topologies. *Sol. Energy* **2019**, *183*, 57–73. [[CrossRef](#)]
4. Hamed, S.B.; Ben Hamed, M.; Sbita, L.; Bajaj, M.; Blazek, V.; Prokop, L.; Misak, S.; Ghoneim, S.S.M. Robust Optimization and Power Management of a Triple Junction Photovoltaic Electric Vehicle with Battery Storage. *Sensors* **2022**, *22*, 6123. [[CrossRef](#)]
5. Aggarwal, S.; Bajaj, M.; Singh, A.K. Analysis of Electric Vehicle Charging Station Allocation in Deregulated Electric Power System. In Proceedings of the 2020 IEEE 9th Power India International Conference (PIICON), Sonapat, India, 28 February–1 March 2020; pp. 1–6. [[CrossRef](#)]
6. Belik, M. Optimisation of Energy Accumulation for Renewable Energy Sources. *Renew. Energy Power Qual. J.* **2021**, *19*, 205–210. [[CrossRef](#)]
7. Mohanty, S.; Panda, S.; Parida, S.M.; Rout, P.K.; Sahu, B.K.; Bajaj, M.; Zawbaa, H.M.; Kumar, N.M.; Kamel, S. Demand side management of electric vehicles in smart grids: A survey on strategies, challenges, modeling, and optimization. *Energy Rep.* **2022**, *8*, 12466–12490. [[CrossRef](#)]
8. Poullikkas, A. Sustainable options for electric vehicle technologies. *Renew. Sustain. Energy Rev.* **2015**, *41*, 1277–1287. [[CrossRef](#)]
9. Andwari, A.M.; Pesiridis, A.; Rajoo, S.; Martinez-Botas, R.; Esfahanian, V. A review of Battery Electric Vehicle technology and readiness levels. *Renew. Sustain. Energy Rev.* **2017**, *78*, 414–430. [[CrossRef](#)]
10. Locment, F.; Sechilariu, M. Modeling and Simulation of DC Microgrids for Electric Vehicle Charging Stations. *Energies* **2015**, *8*, 4335–4356. [[CrossRef](#)]
11. Dharavat, N.; Sudabattula, S.K.; Velamuri, S.; Mishra, S.; Sharma, N.K.; Bajaj, M.; Elgamli, E.; Shouran, M.; Kamel, S. Optimal Allocation of Renewable Distributed Generators and Electric Vehicles in a Distribution System Using the Political Optimization Algorithm. *Energies* **2022**, *15*, 6698. [[CrossRef](#)]
12. Shanmugam, Y.; Narayanamoorthi, R.; Vishnuram, P.; Savio, D.; Yadav, A.; Bajaj, M.; Nauman, A.; Khurshaid, T.; Kamel, S. Solar-powered five-leg inverter-driven quasi-dynamic charging for a slow-moving vehicle. *Front. Energy Res.* **2023**, *11*, 185. [[CrossRef](#)]
13. Monteiro, V.; Oliveira, C.F.; Afonso, J.L. Experimental Validation of a Bidirectional Multilevel dc–dc Power Converter for Electric Vehicle Battery Charging Operating under Normal and Fault Conditions. *Electronics* **2023**, *12*, 851. [[CrossRef](#)]
14. Subramaniam, U.; Vavilapalli, S.; Padmanaban, S.; Blaabjerg, F.; Holm-Nielsen, J.B.; Almakhles, D. A Hybrid PV-Battery System for ON-Grid and OFF-Grid Applications—Controller-In-Loop Simulation Validation. *Energies* **2020**, *13*, 755. [[CrossRef](#)]
15. Savio, D.A.; Juliet, V.A.; Chokkalingam, B.; Padmanaban, S.; Holm-Nielsen, J.B.; Blaabjerg, F. Photovoltaic Integrated Hybrid Microgrid Structured Electric Vehicle Charging Station and Its Energy Management Approach. *Energies* **2019**, *12*, 168. [[CrossRef](#)]
16. Pachauri, N.; Thangavel, V.; Suresh, V.; Kantipudi, M.P.; Kotb, H.; Tripathi, R.N.; Bajaj, M. A Robust Fractional-Order Control Scheme for PV-Penetrated Grid-Connected Microgrid. *Mathematics* **2023**, *11*, 1283. [[CrossRef](#)]
17. Torreglosa, J.P.; García-Triviño, P.; Fernández-Ramírez, L.M.; Jurado, F. Decentralized energy management strategy based on predictive controllers for a medium voltage direct current photovoltaic electric vehicle charging station. *Energy Convers. Manag.* **2016**, *108*, 1–13. [[CrossRef](#)]
18. Guerrero, J.M.; Chandorkar, M.; Lee, T.-L.; Loh, P.C. Advanced Control Architectures for Intelligent Microgrids—Part I: Decentralized and Hierarchical Control. *IEEE Trans. Ind. Electron.* **2012**, *60*, 1254–1262. [[CrossRef](#)]
19. Bajaj, M.; Flah, A.; Alowaidi, M.; Sharma, N.K.; Mishra, S.; Sharma, S.K. A Lyapunov-Function Based Controller for 3-Phase Shunt Active Power Filter and Performance Assessment Considering Different System Scenarios. *IEEE Access* **2021**, *9*, 66079–66102. [[CrossRef](#)]
20. Mojumder, R.H.; Antara, F.A.; Hasanuzzaman, M.; Alamri, B.; Alsharef, M. Electric Vehicle-to-Grid (V2G) Technologies: Impact on the Power Grid and Battery. *Sustainability* **2022**, *14*, 13856. [[CrossRef](#)]
21. Yao, L.; Damiran, Z.; Lim, W.H. A fuzzy logic based charging scheme for electric vehicle parking station. In Proceedings of the 2016 IEEE 16th International Conference on Environment and Electrical Engineering (EEEIC), Florence, Italy, 7–10 June 2016; pp. 1–6.
22. Ma, T.; Mohammed, O. Economic analysis of real-time large scale PEVs network power flow control algorithm with the consideration of V2G services. In Proceedings of the 2013 IEEE Industry Applications Society Annual Meeting, Lake Buena Vista, FL, USA, 6–11 October 2013; pp. 1–8.
23. Chandrasekar, B.; Nallaperumal, C.; Padmanaban, S.; Bhaskar, M.S.; Holm-Nielsen, J.B.; Leonowicz, Z.; Masebinu, S.O. Non-isolated high-gain triple port DC–DC buck-boost converter with positive output voltage for photovoltaic applications. *IEEE Access* **2020**, *8*, 113649–113666. [[CrossRef](#)]
24. Belik, M. Simulation of photovoltaic panels thermal features. In Proceedings of the 2017 18th International Scientific Conference on Electric Power Engineering, EPE 2017, Kouty nad Desnou, Czech Republic, 17–19 May 2017.
25. Kakouche, K.; Rekioua, T.; Mezani, S.; Oubelaid, A.; Rekioua, D.; Blazek, V.; Prokop, L.; Misak, S.; Bajaj, M.; Ghoneim, S.S.M. Model Predictive Direct Torque Control and Fuzzy Logic Energy Management for Multi Power Source Electric Vehicles. *Sensors* **2022**, *22*, 5669. [[CrossRef](#)] [[PubMed](#)]

26. Sureshbabu; Padmanabhan, S.; Subramanian, G.; Stonier, A.A.; Peter, G.; Ganji, V. Design and analysis of a photovoltaic-powered charging station for plug-in hybrid electric vehicles in college campus. *IET Electr. Syst. Transp.* **2022**, *12*, 358–368. [[CrossRef](#)]
27. Sbordone, D.; Bertini, I.; Di Pietra, B.; Falvo, M.; Genovese, A.; Martirano, L. EV fast charging stations and energy storage technologies: A real implementation in the smart micro grid paradigm. *Electr. Power Syst. Res.* **2015**, *120*, 96–108. [[CrossRef](#)]
28. Fotouhi, A.; Propp, K.; Auger, D.J. Electric vehicle battery model identification and state of charge estimation in real world driving cycles. In Proceedings of the 2015 7th Computer Science and Electronic Engineering Conference (CEECE), Colchester, UK, 24–25 September 2015; pp. 243–248.
29. Sheng, H.; Xiao, J. Electric vehicle state of charge estimation: Nonlinear correlation and fuzzy support vector machine. *J. Power Sources* **2015**, *281*, 131–137. [[CrossRef](#)]
30. Justin, F.; Peter, G.; Stonier, A.A.; Ganji, V. Power Quality Improvement for Vehicle-to-Grid and Grid-to-Vehicle Technology in a Microgrid. *Int. Trans. Electr. Energy Syst.* **2022**, *2022*, 2409188. [[CrossRef](#)]
31. Panchanathan, S.; Vishnuram, P.; Rajamanickam, N.; Bajaj, M.; Blazek, V.; Prokop, L.; Misak, S. A Comprehensive Review of the Bidirectional Converter Topologies for the Vehicle-to-Grid System. *Energies* **2023**, *16*, 2503. [[CrossRef](#)]
32. He, P.; Khaligh, A. Comprehensive Analyses and Comparison of 1 kW Isolated DC–DC Converters for Bidirectional EV Charging Systems. *IEEE Trans. Transp. Electrif.* **2016**, *3*, 147–156. [[CrossRef](#)]
33. Ashique, R.H.; Salam, Z.; Aziz, M.J.B.A.; Bhatti, A.R. Integrated photovoltaic-grid dc fast charging system for electric vehicle: A review of the architecture and control. *Renew. Sustain. Energy Rev.* **2017**, *69*, 1243–1257. [[CrossRef](#)]
34. Liu, J.; Huang, X.; Hong, Y.; Li, Z. Coordinated Control Strategy for Operation Mode Switching of DC Distribution Networks. *J. Mod. Power Syst. Clean Energy* **2020**, *8*, 334–344. [[CrossRef](#)]
35. Liu, Y.; Tang, Y.; Shi, J.; Shi, X.; Deng, J.; Gong, K. Application of Small-Sized SMES in an EV Charging Station with DC Bus and PV System. *IEEE Trans. Appl. Supercond.* **2015**, *25*, 1–6. [[CrossRef](#)]
36. Dragičević, T.; Sučić, S.; Vasquez, J.C.; Guerrero, J.M. Flywheel-based distributed bus signaling strategy for the public fast charging station. *IEEE Trans. Smart Grid* **2014**, *5*, 2825–2835. [[CrossRef](#)]
37. Al Sumarmad, K.A.; Sulaiman, N.; Wahab, N.I.A.; Hizam, H. Energy Management and Voltage Control in Microgrids Using Artificial Neural Networks, PID, and Fuzzy Logic Controllers. *Energies* **2022**, *15*, 303. [[CrossRef](#)]
38. Al Sumarmad, K.A.; Sulaiman, N.; Wahab, N.I.A.; Hizam, H. Microgrid Energy Management System Based on Fuzzy Logic and Monitoring Platform for Data Analysis. *Energies* **2022**, *15*, 4125. [[CrossRef](#)]
39. Faisal, M.; Hannan, M.A.; Ker, P.J.; Lipu, M.S.H.; Uddin, M.N. Fuzzy-Based Charging–Discharging Controller for Lithium-Ion Battery in Microgrid Applications. *IEEE Trans. Ind. Appl.* **2021**, *57*, 4187–4195. [[CrossRef](#)]
40. Hussain, S.; Ahmed, M.A.; Lee, K.-B.; Kim, Y.-C. Fuzzy Logic Weight Based Charging Scheme for Optimal Distribution of Charging Power among Electric Vehicles in a Parking Lot. *Energies* **2020**, *13*, 3119. [[CrossRef](#)]
41. Baramadeh, M.Y.; Abouelela, M.A.A.; Alghuwainem, S.M. Maximum Power Point Tracker Controller Using Fuzzy Logic Control with Battery Load for Photovoltaics Systems. *Smart Grid Renew. Energy* **2021**, *12*, 163–181. [[CrossRef](#)]

Disclaimer/Publisher’s Note: The statements, opinions and data contained in all publications are solely those of the individual author(s) and contributor(s) and not of MDPI and/or the editor(s). MDPI and/or the editor(s) disclaim responsibility for any injury to people or property resulting from any ideas, methods, instructions or products referred to in the content.